International Journal of Scientific Engineering and Applied Science (IJSEAS) - Volume-1, Issue-4,July 2015
ISSN: 2395-3470
www.ijseas.com

CARTOON-TEXTURE IMAGE DECOMPOSITION USING BLOCK WISE LOW-RANK TEXTURE CHARACTERIZATION

Meenakshi Tummala[1], Dr.Y.Venkateswarulu[2], Dr. U Ravi Babu[3]

[1]Mtech Student ,CSE, Giet Engineering College, Rajahmundry, A,P, India
[2]Professor and HOD, Dept of CSE, Giet Engineering College, Rajahmundry, A,P, India
Professor, Dept of CSE, MREC(A)

ABSTRACT

We propose anImagedecomposition method that can viably deteriorates a picture into its cartoon and composition segments by utilizing a portrayal of surface. The portrayal rests on our perception that the surface segment appreciates a blockwise low-rank nature with conceivable cover and shear, on the grounds that composition, all in all, is universally different however by regional standards decently designed. We set up a cartoon composition disintegration demonstrate as a raised improvement issue, where the synchronous estimation of the toon and surface parts from a given picture or debased perception is executed by minimizing the aggregate variety and BNN. Moreover, the model can deal with different sorts of corruption happening in picture handling, including smear + missing pixels with a few sorts of clamor. By revising the issue through variable part, the supposed rotating heading strategy for multipliers gets to be relevant, bringing about an effective algorithmic answer for the issue. Numerical illustrations outline that the proposed model is exceptionally particular to examples of composition, which improves it deliver results than cutting edge disintegration models.

Index Terms-Cartoon-texturedecompo - sition, convexoptimization, image restoration, low-rank interpretation, texturecharacterization.

INTRODUCTION:

Oneof the most important and longstanding problemsin image processing is image decomposition, whichplays a central role in a wide range of applications suchas image restoration, biomedical engineering, astronomicalimaging, remote sensing, pattern recognition, and computervision. In image decomposition, an image is often modeled asthe superposition of two meaningful components, namely, thecartoon component and the texture component. The cartoon component is the piecewise-smooth part having the global structural information of the image, and the texture component is the locally-patterned oscillating part. A popular and effective strategy to achieve such decomposition is to formulate it as a convex optimization problem, in which the components are characterized by appropriate convex priors. Indeed, under a variety of scenarios, image decomposition based on the said strategy has been extensively studied[1-10].

Very recently, Schaeffer and Osher proposed to interpret texture using what is called the Low Patch-Rank [11]. Their approach is mainly motivated by Robust PCA [12]–[15] and models the texture

component as an alignment of patches which are almost linearly dependent. For its special capability of capturing patterned structure, their cartoon-texture decomposition model, which we shall refer to as the LPR model, is shown to be superior to other existing ones in terms of texture characterization and at the same time outperforms the non-local TV regularization [16]–[18] in the restoration of well-textured images. However, it is also true that, because of its fully-global (not locally-adaptive) nature, the LPR model is not much suitable for characterizing

texture having various different patterns, which is typical in many images, and thereby sometimes producing undesirable patterned-artifacts

The very nature of BNN in the proposed model not only realizes a reasonable texture characterization by its low-rank interpretation but also overcomes the limitation of the LPR model by its local adaptivity. In addition, the proposed model is designed to accept various degradation scenarios, including blur + missing pixels with noise. Such a scenario was considered in a recent study under a Gaussian noise assumption. Notably the proposed model can also handle several non-Gaussian noise cases in a unified way with the associated convex optimization problem solvable using proximal splitting techniques.

The rest of the paper is organized into 3 sections section 2 describe the proposed method and results are discusswed in section 4 and conclusions are given in section 4

PROPOSED METHOD: IMAGE DECOMPOSITION MODEL

This section is devoted to the proposal of an image decomposition model as a convex optimization problem, where we characterize the texture component using multiple BNN with different shear angles and present a guarantee of the existence of a minimizer. An optimization scheme based on ADMM for the proposed model is also provided with its convergence property and efficient implementation.

Formulation: Consider to the estimation of ideal cartoon and texture components C, T∈ R^N (N= $n_v n_h$, $n_v \times n_h$ corresponds tothe image size) from an observation **v**:= ϱ([**u**org)∈R^M(M∈N), where $\mathbf{u}_{org}$=C + T∈R^N is an original image,□∈ $R^{M\times N}$a linear observation operator representing somedeterioration process (e.g., blur and/or missing pixels), andN : $R^M \rightarrow R^M$a noise contamination being not necessarilyadditive. The proposed cartoon-texture decomposition (possibly with degradation) is then formulated as follows.

(Cartoon-texture decomposition using BNN)

$$\underset{\mathbf{c}\in\mathbb{R}^N,\mathbf{t}_k\in\mathcal{Z},\mathbf{c}+\sum_{k=1}^K \mathbf{t}_k\in\mathcal{D}}{\text{Minimize}} \mathcal{J}_{\text{obj}},$$

$$\mathcal{J}_{\text{obj}} := \lambda\|\mathbf{c}\|_{\text{TV}} + \sum_{k=1}^K \|\mathbf{t}_k\|_{\text{mBNN}}^{\mathbf{w},\delta,\boldsymbol{\theta}_k} + \mathcal{F}_{\mathbf{v}}(\Phi(\mathbf{c}+\sum_{k=1}^K \mathbf{t}_k)),$$

where $\mathbf{t}_k$(k = 1, . . . , K) are the sub-texture components, Z ⊂ RN is the set of all zero-average vectors defined by Z := {**x** ∈ R^N | N_i=1^{x}i$^=$0}, D ⊂R^N a (normalized) dynamic range constraint given by D := {**x**∈ RN | x_i∈ [0, 1] (i=1, . . . , N)}, λ∈R++, and F**v** ∈ 0(R^M) is a certain datafidelity function regarding the observation **v**, the proximity operator of which is available. Note that the texture component **T** is modeled as **T**:=$_k$K$_=$1^{t}k, where each $\mathbf{t}_k$is characterized by BNN with a different shear angle, i.e., consisting of patterns extending in a specific direction.

(a) Noiseless case: Since $\mathbf{v} = \mathbf{u}_{org}$, a suitable fidelity is $F_{\mathbf{v}}(\mathbf{x}) = \iota C_{\mathbf{v}}(\mathbf{x})$, where $\iota C_{\mathbf{v}}$is the indicator function of the closed convex set $C_{\mathbf{v}} := \{\mathbf{x} \in R^M | \mathbf{x} = \mathbf{v}\}$. The associated proximity operator is given by $\text{prox}\gamma F_{\mathbf{v}}(\mathbf{x}) = PC_{\mathbf{v}}(\mathbf{x}) = \mathbf{v}$, where PC stands for the metric projection onto a nonempty closed convex set CI

(b) Gaussian noise case: A standard choice is to use the additive _2 fidelity: $F_{\mathbf{v}} := \mu/2\| \cdot - \mathbf{v}\|2/2(\mu \in R_{++}$, and $\|\cdot\|_2$ denotes the ℓ2 norm), with the associated proximityoperator given by $\text{prox}\gamma F_{\mathbf{v}}(\mathbf{x}) = \mu\gamma\mathbf{v}+\mathbf{x}\mu\gamma+1$. An alternativechoice is the constrained type fidelity: $F\mathbf{v}(\mathbf{x}) := \iota B2\mathbf{v},\varepsilon(\mathbf{x})$,where $B^2_{\mathbf{v},\varepsilon} := \{\mathbf{x} \in R^M | \|\mathbf{x} - \mathbf{v}\|2 \leq \varepsilon\}$ ($\varepsilon \in R_{++}$).The associated proximity operator is the metric projectiononto $B^2_{\mathbf{v},\varepsilon}$, i.e., $\text{prox}\gamma F_{\mathbf{v}}(\mathbf{x}) = P_{B^2_{\mathbf{v},\varepsilon}}(\mathbf{x}) = \mathbf{x}$, if $\mathbf{x} \in B^2\mathbf{v},\varepsilon;\mathbf{v} + \varepsilon(\mathbf{x}-\mathbf{v})/ \|\mathbf{x}-\mathbf{v}\|2$, otherwise.

(c) Impulsive noise case: It is well known that using the ℓ1 norm as fidelity measure is robust to impulsive noise contamination. The additive ℓ1 fidelity is given by $F\mathbf{v} := \mu\| \cdot - \mathbf{v}\|_1$ ($\mu \in R_{++}$, and $\|\cdot\|_1$ denotes the ℓ1 norm), the proximity operator of which can be computed by the soft-thresholding: for i= 1, . . . , M, by

$$[\text{prox}_{\gamma F_{\mathbf{v}}}(\mathbf{x})]_i = v_i + \text{sgn}(x_i - v_i)\max\{|x_i - v_i| - \gamma\mu, 0\}$$

wheresgn denotes the signum function. As in (a), the constrained type alternative is $F_{\mathbf{v}}(\mathbf{x}) := \iota B_1\mathbf{v},\varepsilon(\mathbf{x})$, where $B_1\mathbf{v},\varepsilon := \{\mathbf{x} \in R^M | \|\mathbf{x} - \mathbf{v}\|1 \leq \varepsilon\}$. The associated proximity operator can be computed efficiently by a fast ℓ1 ball projection algorithm [19].

(d) Poisson noise case: It has been shown that under Poisson noise contamination, the so-called generalized KulbackLeibler divergence is suitable for F**v**. The definition and the computation of the associated proximity operator can be found in [20].

RESULTS AND DISCUSSIONS

We examine the effectiveness of the proposed cartoon texture decomposition model in several scenarios. All experiments were performed using MATLAB (R2013a), on a Windows 7 (64bit) desktop computer with an Intel Core i7 2.8 GHz processor and 8.0 GB of RAM. The dynamic range of test images (256 × 256) are normalized to [0, 1].In (5), we use $\gamma = 0.1$ and $\mathbf{s}(0) = \mathbf{d}(0) = \mathbf{0}$, and for the stopping criterion, adopt $\_\mathbf{r}(n+1) - \mathbf{r}(n)\_2 < 0.1$. The tolerance value and max iteration number of the preconditioned conjugate gradient method are set to 1.0×10^{-6} and 20, respectively.

Decomposition

Here we consider pure decomposition, i.e., no degradation,to analyze the characteristics of the proposed model. In thiscase, the observation **v** is the original image **u**org, so that asuitable data-fidelity function is ι**C****v**.We first use the synthesized image Sakura, shown in thetop left of Fig. 1, to give a clear insight into the behavior ofthe proposed decomposition, i.e., the sub-texture separationcapability. For reference, we also apply the nuclear normmodel, i.e., simply using the nuclear norm (i.e., BNN withk = 1, $\boldsymbol{\theta}1 = (*, 0)$, and mv = δv= nv ,mh= δh= nh)as a prior for texture component, and the LPR model tothe image, where we optimize them by using the proposedalgorithm modified for these models.7 We choose the blocksize **m** and the shift step number **δ** of

BNN as (16, 16) and(8, 8), and the number of sub-texture components is set toK = 3. In each model, the parameter controlling the balancebetween TV and texture prior (the nuclear norm, LPR or BNN)is selected in such a way that the decomposed cartoon and texturecomponents are closest to the oracle ones in the sense ofthe Euclidean distance. Note that such parameter optimization is only available when we use synthesized images.

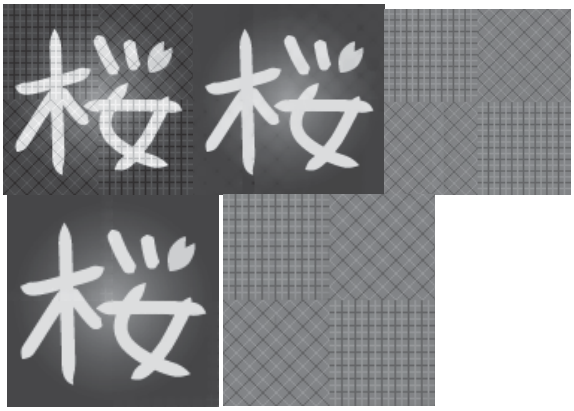

(a) (b) (c) (d) (e)

Fig1: Pure decomposition results using the synthesized imagea) original Image b) cartoon Image c) texture by cartoon d0 cartoon LPR e0 texture by LPR

As can be seen in Fig. 1, all the models produce reasonablecartoon-texture decompositions. This is because theSakura image consists of both simple cartoon and texture,and thus can be easily decomposed. We observe that patternsextending in different directions are extracted as sub-texturecomponents in an almost completely-separated manner byusing the proposed model with the exact shear angle of 45◦,implying that the proposed texture characterization based onBNN with different shear angles appropriately works. Wealso show decomposition results of using shear angles whichdo not exactly match the directions in the third and fourth

rows of Fig. 1. As expected, the larger difference of shearangle from the exact one leads to the more different sub-textureseparation. One may think that, in the case of simpletexture such as in the Sakura image, similar sub-texturecomponents can be generated by applying some directionalanalysis transform (e.g., directional wavelet) to the texturecomponent obtained by the nuclear or LPR model. Actually,this kind of things may be possible by using a combinationof some suitable methods, but, compared with such sequentialmethods, the use of the proposed model has the followingadvantages: i) To begin with, extracting a reasonable texturecomponent from a given image is difficult and important,and indeed, the succeeding experimental results demonstratethat the proposed model is more suitable to this task thanexisting models; ii) The proposed model provides cartoon-texturedecomposition and sub-texture separation in a unifiedmanner, i.e., by just solving one convex optimization problem,so that we can guarantee the optimality in the sense of themodel.Next we compare the proposed model with the LPR onevia non-synthesized images Barbara and House [the top leftof Fig. 2(a) and (b)]. Note that, in this case, the oracledecomposition of each image is unavailable, so that we cannotoptimize the parameters of the models as in the case of Sakura.To conduct a fair comparison, we produce decompositionresults by the use of the LPR model with different

parametersettings, in order to illustrate the superiority of the proposedmodel in terms of extracting patterned texture.The results are depicted in Fig. 3 (from top to bottom,cartoon component, texture component, and their close-ups).In Fig. 3(b), we see that the texture component extracted bythe proposed model only contains patterned fabric and nocontours, implying that our model is very selective to patterns.Such decomposition cannot be achieved by the LPR modelas shown in Fig. 3(a), where if we set parameters to extractsufficient texture then the resulting texture component containscontours (left), and if set to not contain contours then patternedtexture remains in the cartoon component (right). In the caseof House, our texture component [Fig. 3(d)] exhibits patterned

Structure like roof tiles and windows but there are very fewnon-patterned objects, which also indicates the selectivity ofthe proposed model. By contrast, the LPR model with anyparameter setting does not lead to a decomposition similarto the proposed one [Fig. 3(c)]. We also present the correspondingsub-texture components obtained by the proposedmodel in Fig. 5, in which we observe that patterns extendingin different directions are extracted separately. These results verify a special capability of BNN, namely, that of capturingglobally dissimilar but locally well-patterned nature of texture.

The required iteration number and CPU time for the proposedmodel on Barbara are 66 and 37[sec], and those for the LPRmodel 151 and 32[sec], being almost the same on House.

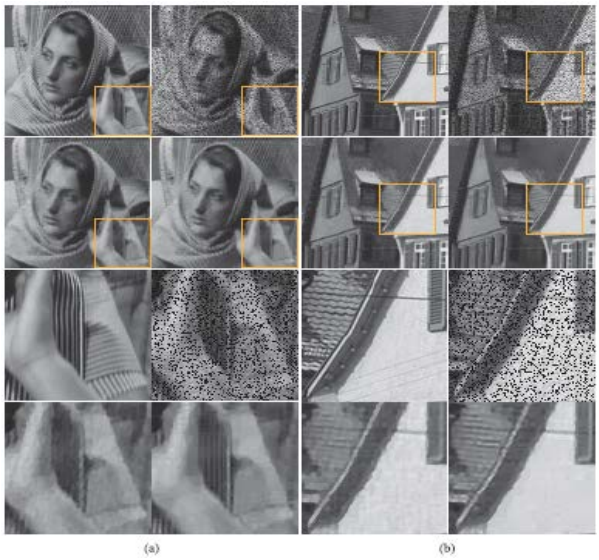

Fig. 2: Comparison of the results of deblurring (3 × 3 Gaussian blur) with 20% missing pixels for each group, from left to right, top to bottom: original, observation, LPR's result, our result, and their close-ups): The proposed model is locally-adaptive, and hence it can restore fine texture without generating patterned artifacts observed in the LPR's results. (a) Results on Barbara. (b) Results on House.

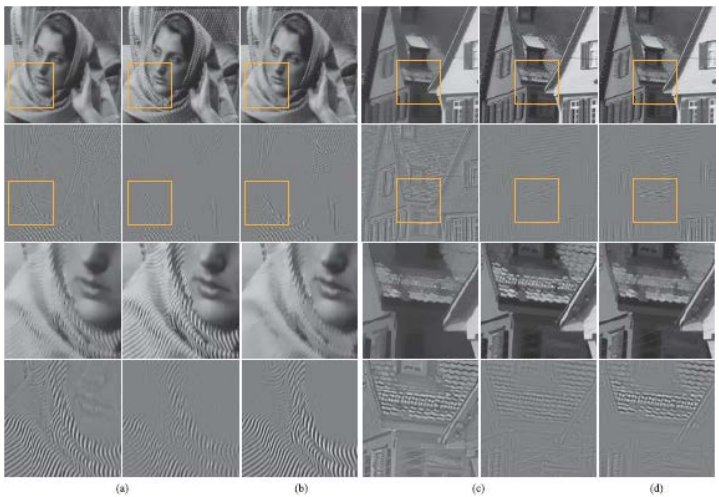

Fig. 4. Comparison of decomposition results (for each column, from top to bottom, cartoon; texture; close-up of cartoon; close-up of texture): The proposed model extracts

sufficient texture without containing edges and contours, which cannot be achieved by the LPR model using any parameter setting. (a) LPR with two different parameter settings. (b) Proposed. (c) LPR with two different parameter settings. (d) Proposed.

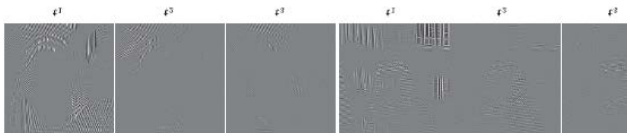

Fig. 5: Sub-texture components of the results in Fig. 3(b) and (d): Patterns extending in different directions are extracted separately. Note that they are magnified by a factor of three for visibility.

We plot in Fig. 6 the improvement of PSNR and SSIM by the proposed model and the LPR model from the best average performance of the G-norm model [12], where we examine the proposed method using different block sizes and shift step numbers with respect to varying λ in (3). From the results in Fig. 7, the best average performance of the proposed model with all the block sizes and shift step numbers exceed those of the G-norm and LPR models, which implies that the proposed model agrees well with a variety of images compared to the other models.

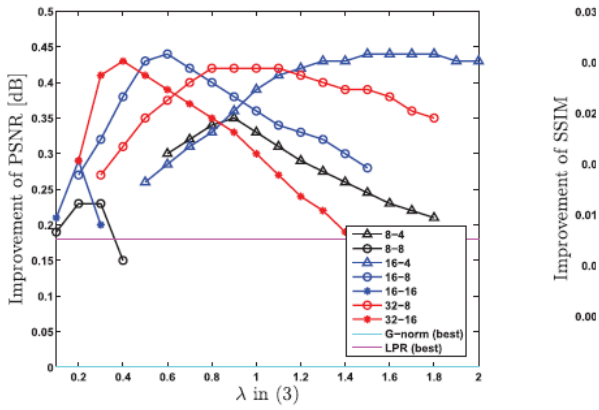

Fig. 6. Improvement of PSNR [dB] and SSIM by the proposed model and the LPR model from the best average performance of the G-norm (averaged over 200 images) with respect to varying λ in (3): The legend of black, blue and red lines indicate the block size and shift step number of the proposed method, e.g., 16 − 8 means mv = mh= 16 and δv= δh= 8.

Observations from the proposed method:

a) The value of lambda giving the best average performance depends on the block size and shift step number, as indicated in Fig. 6. Specifically, first, the more redundant setting, i.e., the smaller shift step number, requires the larger λ to achieve the best average performance, implying that the value of BNN is proportional to the redundancy rate (mvmh)/(δvδh). Second, based on one redundancy rate, the smaller block size needs a larger λ for the best average performance, which means the increase of the number of blocks leads to the increase of the value of BNN.
b) Among all the block sizes, the smallest one (mv = mh= 8) results in the worst performance, as observed in Fig. 6. This would be because an excessively small block size cannot capture and reconstruct patterns well.
c) The non-overlapped settings (the lines of ‘8-8’ and ‘16-16’ in Fig. 7) perform poorly, which agrees with the intuition that it tends to produce undesirable blocky effects. Basically, a higher overlap level leads to a better performance but with a more expensive computational cost.
d) It is natural to suppose that a large K leads to a more accurate

characterization of patterns extending in various directions, and thus results in a better restoration. The experimental results in Table II match this expectation. At the same time, the computational complexity grows because of the increase in the number of the separated components.

CONCLUSIONS:

We have proposed a cartoon-texture decomposition model with a novel texture prior named the Block Nuclear Norm (BNN). Using BNN, our model interprets the texture component as the combination of blockwise low-rank matrices with possible overlap and shear, which leads to a suitable characterization of globally dissimilar but locally well-patterned nature of texture. The convex optimization problem associated with the proposed model is efficiently solved by ADMM. Numerical examples demonstrate its effectiveness both in pure decomposition and restoration. Future works include an efficient implementation based on the blockwise nature of BNN, extension to color image decomposition with the incorporation of the combination with more involved data-fidelity constraints under various scenarios of noise contamination, and the incorporation into hierarchical convex optimization for selecting a better pair of cartoon and texture components among all the solutions to the proposed model.

REFERENCES:

1. Rudin, S. Osher, and E. Fatemi, “Nonlinear total variation based noise removal algorithms,” Phys. D, vol. 60, nos. 1–4, pp. 259–268, 1992.

2. Y. Meyer, Oscillating Patterns in Image Processing and Nonlinear Evolution Equations: The Fifteenth Dean Jacqueline B. Lewis Memorial Lectures, vol. 22. Providence, RI, USA: AMS, 2001.

3. L. Vese and S. Osher, “Modeling textures with total variation minimization and oscillating patterns in image processing,” J. Sci. Comput., vol. 19, no. 1, pp. 553–572, 2003.

4. S. Osher, A. Solè, and L. Vese, “Image decomposition and restoration using total variation minimization and the H−1 norm,” Multiscale Model. Simul., vol. 1, no. 3, pp. 349–370, 2003.

5. M. Bertalmio, L. Vese, G. Sapiro, and S. Osher, “Simultaneous structure and texture image inpainting,” IEEE Trans. Image Process., vol. 12, no. 8, pp. 882–889, Aug. 2003.

6. J.-F. Aujol, G. Aubert, L. Blanc-Fèrau, and A. Chambolle, “Image decomposition into a bounded variation component and an oscillating component,” J. Math. Imag. Vis., vol. 22, no. 1, pp. 71–88, 2005.

7. J.-F. Aujol and A. Chambolle, “Dual norms and image decomposition models,” Int. J. Comput. Vis., vol. 63, no. 1, pp. 85–104, 2005.

8. J. L. Starck, M. Elad, and D. L. Donoho, “Image decomposition via the combination of sparse representations and a variational approach,” IEEE Trans. Image Process., vol. 14, no. 10, pp. 1570–1582, Oct. 2005.

9. I. Daubechies and G. Teschke, "Variational image restoration by means of wavelets: Simultaneous decomposition, deblurring, and denoising," Appl. Comput. Harmon. Anal., vol. 19, no. 1, pp. 1–16, Jul. 2005.

10. J.-F. Aujol, G. Gilboa, T. Chan, and S. Osher, "Structure-texture image decomposition—Modeling, algorithms, and parameter selection," Int. J. Comput. Vis., vol. 67, no. 1, pp. 111–136, 2006.

11. H. Schaeffer and S. Osher, "A low patch-rank interpretation of texture," SIAM J. Imag. Sci., vol. 6, no. 1, pp. 226–262, 2013.

12. Y. Peng, A. Ganesh, J. Wright, and Y. Ma, "RASL: Robust alignment by sparse and low-rank decomposition for linearly correlated images," in Proc. IEEE Conf. CVPR, Jun. 2010, pp. 7633–770.

13. S. Gandy and I. Yamada, "Convex optimization techniques for the efficient recovery of a sparsely corrupted low-rank matrix," J. Math. Ind., vol. 2, pp. 147–156, Aug. 2010.

14. E. J. Candès, X. Li, . Ma, and J. Wright, "Robust principal component analysis?" J. ACM, vol. 58, no. 3, pp. 1–22, 2011.

15. Z. Zhang, X. Liang, A. Ganesh, and Y. Ma, "TILT: Transform invariant low-rank textures," Int. J. Compt. Vis., vol. 99, no. 1, pp. 1–24, 2012.

16. G. Gilboa and S. Osher, "Nonlocal linear image regularization and supervised segmentation," Multiscale Model. Simul., vol. 6, no. 2, pp. 595–630, 2007.

17. G. Gilboa and S. Osher, "Nonlocal operators with applications to image processing," Multiscale Model. Simul., vol. 7, no. 3, pp. 1005–1028, 2009.

18. X. Zhang, M. Burger, X. Bresson, and S. Osher, "Bregmanized nonlocal regularization for deconvolution and sparse reconstruction," SIAM J. Imag. Sci., vol. 3, no. 3, pp. 253–276, 2010.

19. J. Duchi, S. S. Shwartz, Y. Singer, and T. Chandra, "Efficient projections onto the _1-ball for learning in high dimensions," in Proc. 25th ICML, 2008, pp. 272–279.

20. P. L. Combettes and J.-C. Pesquet, "A Douglas-Rachford splitting approach to nonsmooth convex variational signal recovery," IEEE J. Sel. Topics Signal Process., vol. 1, no. 4, pp. 564–574, Dec. 2007.